International Journal of Mechanical, Industrial and Aerospace Sciences
ISSN: 2517-9950
Vol:3, No:8, 2009

A Model for Study of the Defects in Rolling Element Bearings at Higher Speed by Vibration Signature Analysis

Abhay Utpat, R. B. Ingle, and M. R. Nandgaonkar

***Abstract*—**The vibrations produced by a single point defect on various parts of the bearing under constant radial load are predicted by using a theoretical model. The model includes variation in the response due to the effect of bearing dimensions, rotating frequency distribution of load. The excitation forces are generated when the defects on the races strike to rolling elements. In case of the outer ring defect, the pulses generated are with periodicity of outer ring defect frequency where as for inner ring defect, the pulses are with periodicity of inner ring defect frequency. The effort has been carried out in preparing the physical model of the system. Different defect frequencies are obtained and are used to find out the amplitudes of the vibration due to excitation of the bearing parts. Increase in the radial load or severity of the defect produces a significant change in bearing signature characteristics**.**

***Keywords*—**Condition monitoring, defect frequency, rolling element, vibration response.

I. Introduction

THE main source of the vibration in the rolling bearing are defects on the races and the rolling element. Vibration transmission through rolling element is investigated in order to aid signal interpretation for using in the condition monitoring [1,2].Rolling element bearings are found in two basic configurations depending upon whether they use ball or roller type elements. The most popular rolling bearing is single row deep groove ball bearing and this will be considered for the case of radial contact. Vibration response measurement is an important and effective technique for the detection of defects in rolling element bearings [3]. Even a geometrically perfect bearing under radial load may generate vibration due to time varying contact forces which exist between the various bearing components**.** However, the nature of vibration response changes with the presence of defects in various bearing elements. The localized bearing defects include cracks, pits caused primarily due to fatigue on the rolling surfaces. When such a defect on one surface strikes it's mating surface, a pulse of short duration is generated which excites vibration of the rotor-bearing system [4-6]. Vibration measurement in both time domain and frequency domain has been utilized for condition monitoring of bearings. The frequency domain approach, which essentially means the spectral analysis of vibration signal, is widely used for bearing defect detection. Many techniques have also been attempted to improve the signal to noise ratio. Prediction of amplitude becomes difficult because of the complex nature of the system resulting from assembly of bearing elements and mounting of the same on the shaft and housing. However, McFadden [1] studied that when a defect in one surface of a rolling bearing strikes another surface, it produces an impulse which may excite resonances in the bearing. As the bearing rotates, these impulses will occur periodically with a frequency which is determined uniquely by the location of the defect, may be it on the inner ring, outer ring, or one of the rolling elements. With large defects and medium operating speeds, most methods of detection will work satisfactorily but at low speeds with small defects, problems arise; Smith [3] describes work on measurements at low speeds and discusses the difficulties which arise. Triaxial vibration measurements were taken at each end of the coupling on the motor and rotor bearing housings. The results indicate that bad bearing has a strong effect on the vibration spectra. The results have demonstrated that each one of these techniques is useful to detect problems in roller bearings. However, very little research has been done to correlate the amplitudes of these spectral components at higher speed with the extent of defect, though such a correlation will be of immense help for diagnostic purpose. There is scope in the study of the bearing signatures at higher speed .This paper emphasis on the development of the mathematical expression related to the amplitude of the vibrations produced due to excitation forces caused by striking of the defect with mating surfaces.

II. Formulation of the Model

For the rotor bearing system subjected to external excitations, number of models are proposed, includes two degree and three degree of freedoms. Researchers proposed three degree of freedom model with spring dashpot system. The model considers the outer race to be rigidly mounted in the housing and the inner race to be rigidly mounted on the

A. Utpat is with the College of Engineering Pandharpur, Maharashtra, India & working as a Ass. Prof. in Mechanical Engineering Department (phone: +91-2186-325781,225083; e-mail: abhayutpat@rediffmail.com).

R. B. Ingle was with Gov.College of Engineering ,Pune, India. He is now as a Prof. in the Department of Mechanical Engineering, Tolani Maritime Institute, Pune,India.(e-mail: rbingle2002@yahoo.com).

M. R. Nandgaonkar is with Gov.College of Engineering ,Pune, India. Working as Asst. Prof. in Mechanical Engineering Department.

shaft and thus neglects the flexural vibration of the races. The rotor bearing system has been modeled with the same consideration in the present work. The extended portion of the shaft from right support bearing is considered as cantilever and test bearing is mounted on the same part for measurement of the radial vibrations.

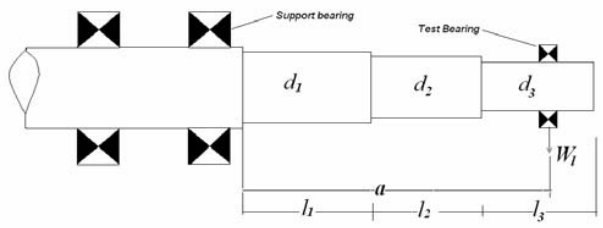

Fig. 1 Shaft for locating the test bearing

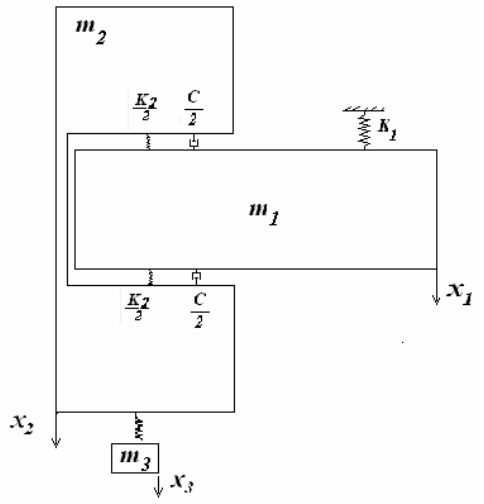

Fig. 2 Physical model of the system

The three DOF system is as shown in Fig. 2. For the rotor bearing system , k_1 is Stiffness of the cantilever portion of the shaft i.e Load at test bearing divided by static deflection at that point. m_1 is sum of mass of inner race & effective mass of extended portion of shaft at point of suspension of test bearing, m_2 is combined effect of mass of housing & mass of outer race, m_3 is sum of mass due to load actually applied & effective mass of the load system, k_3 is stiffness of the loading arrangement and k_2 is linerised bearing stiffness coefficient. i.e.

$$k_2 = P_C / [\delta \max - 0.5Cr] \quad (1)$$

Where, P_C is total load capacity of bearing, δ_{max} is maximum deflection in the direction of the radial load and C_r is dimetral clearance as shown in Fig. 3. Stiffness of the rolling element bearing is important parameter and it depends upon the relationship between maximum rolling element load & the applied load and on the load distribution among various elements. As explained by Harris [8], the load on the rolling element at any angle ϕ from the maximum load direction is given by;

$$Pc = P(\phi) = P_{\max} [1 - (1 - \cos \phi) / 2\varepsilon]^n \text{ for } -\phi_1 < \phi < \phi_1 \quad (2)$$

Where, Load distribution factor, ε = 0.5 (1- Cr / 2 δmax) & n is 3/2 for ball bearing.

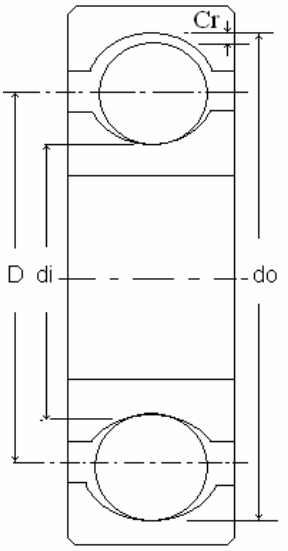

Fig. 3 Dimensions of the ball bearing

At any other position, the $P(\phi)$ is zero. The load zone depends upon the load distribution factor as shown in Fig. 4. The maximum rolling element load is, $P_{\max} = k_{df} \times \delta_{\max}$ where k_{df} is deformation constant as calculated by Harris [8].

The total applied load can be obtained by adding the forces shared by the individual rolling elements in the load zone as shown in Fig. 4. But the value of both $\delta_{\max}$ & ϕ_1 depends upon the magnitude of applied load, P_c. Hence some iterative methods are used for solving above equation. Actually the stiffness coefficient of rolling bearing is Non Linear, but as reviewed by several researchers linearised stiffness coefficient may be assumed if variation from equilibrium due to dynamic forces is small. Also by adding the damping due to each element in the load zone, the total damping coefficient ,c for complete bearing is calculated and is expressed by;

$$c = \sum_{\phi=-\phi_1}^{\phi_1} c_\phi \cos\phi \quad (3a)$$

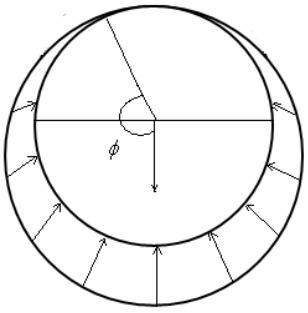

a) $Cr\langle 0, \quad 0.5\langle \varepsilon \langle 1.0, \quad \phi \rangle 90^0$

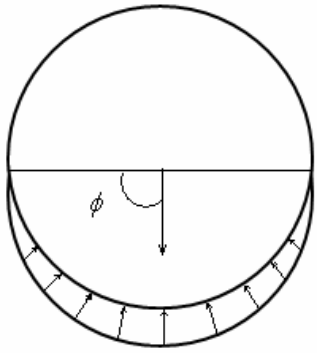

b) $C_r = 0, \varepsilon = 0.5, \phi = \pm 90^0$

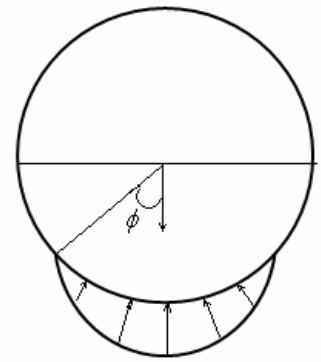

c) $C_r \langle 0,\ 0 \langle \varepsilon \langle 0.5,\ 0 \langle \phi \langle 90^0$

Fig. 4 Load zones according to load distribution factor

Where, c_ϕ = elemental damping constant and

$$c_\phi = \frac{c_i c_o}{c_i + c_o} \tag{3b}$$

Where c_i & c_o = Ball damping coefficient due contact with inner race & outer race respectively [8,10].

III. Differential Equation for the System

For the multi degree of freedom linear system subjected to external excitation, the equation of the motion is given by;

$$m\frac{d^2y}{dx^2} + c\frac{dy}{dx} + kx = Q_i(t) \tag{4}.$$

Where *m, c* and *k* represents mass ,damping and stiffness matrices respectively .Q_i(i =1, 2, 3) is the excitation force due to defect, acting on mass m_i at time *t* and *xi* is the resultant displacement at the same time *t*. However, the force Q_3 is always equal to zero because a defect on a bearing element cannot cause the excitation of a force on mass m_3.

IV. Characteristic Defect Frequencies

The pulses obtained are depend upon the location of the defects whether it is on outer ring, inner ring or on the rolling element. The vibrations of the ball bearing with the defect can be known by emphasizing on the various defect frequencies. The outer ring of the bearing is supposed to be fixed and the inner ring is revolving with the shaft rotation frequency of f_s. With this the frequency of the rotation of the cage f_c and ball revolution frequency, f_b is given by,

$$f_b = \frac{Df_s}{2d}\left[1 - \frac{d^2}{D^2}\cos^2\alpha\right] \tag{a}$$

$$\& \qquad f_c = \frac{f_s}{2}\left[1 - \frac{d}{D}\cos\alpha\right] \tag{b}$$

Where *d* & *D* are the rolling element diameter and pitch diameter respectively. If there is a defect on the inner race, it strikes the balls which are revolving at the speed of f_c. But inner race itself is revolving with the shaft speed *fs*. During the time the bearing makes one complete revolution, the defect comes in to contact with certain numbers of the balls, let Z. Hence inner race defect frequency is given by , $f_i = Z(f_s - f_c)$.

$$\therefore \quad f_i = \frac{Zf_s}{2}\left[1 + \frac{d}{D}\cos\alpha\right] \tag{c}$$

In case of defect on the outer race, Z number of balls strikes the defect with the cage speed of f_c. Hence the outer race defect frequency is Z times the cage frequency which is given by; $f_o = Zf_c$.

$$\therefore \quad f_o = \frac{Zf_s}{2}\left[1 - \frac{d}{D}\cos\alpha\right] \tag{d}$$

In case of the defect on the ball, both outer race and inner race comes in contact with the defect when ball completes one revolution. For this case the frequency of the vibration pulses arising from the defect is calculated by; $f_{bd} = 2f_b$

$$\therefore \quad f_{bd} = \frac{Df_s}{d}\left[1 - \frac{d^2}{D^2}\cos\alpha\right] \tag{e}$$

Fig. 5 shows the cross section of the bearing with various defect frequencies.

V. Vibration Response for Defects at Various Positions

The excitation of the system is caused by pulses generated due to the interaction of the defect with mating elements.

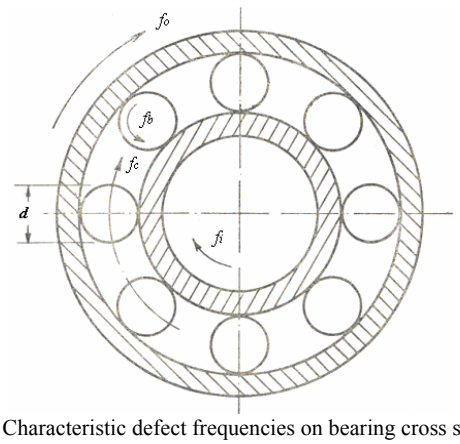

Fig. 5 Characteristic defect frequencies on bearing cross section

Thus,

Q_1 results when pulses are generated on the inner race or mass m_1. Q_2 results when pulses are generated on the outer race or mass m_2. Q_3 is always zero because localized defect on bearing cannot cause any force to be exerted on mass m_3.

The load distribution and generation of the excitation force for radial vibration is as shown in Fig. 6 below.

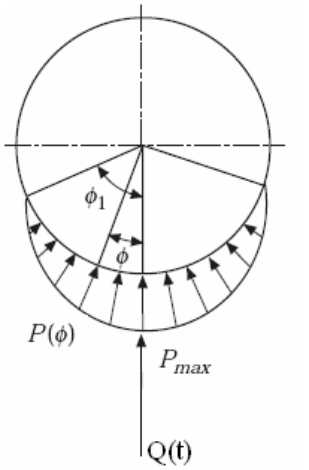

Fig. 6 Load distribution and generation of the excitation force for radial vibration

Hence the excitation force in the direction of the measurement is given by,

$$Q(t) = q(t)P(\phi)\cos\ \phi. \tag{5a}$$

Where, $q(t)$ is generated pulse form and $P(\phi)$ is the load at point of excitation.

The generated wave form is considered as rectangular and periodic in nature, can be expanded in the Fourier series as follows;

$$q(t) = q_o + \sum_s q_s \cos\ ft. \tag{5b}$$

Where,

- f is frequency of generation pulses & depends upon location of the defect.

- q_0 & q_s are Fourier coefficients as given below;

$$q_0 = H\frac{B}{T}$$

& $$q_s = (2H/\pi s)\sin\pi s\frac{B}{T}; \tag{5c}$$

where, H is pulse height & B is pulse width which is ratio of defect width to the relative velocity between mating surfaces, υ_r and is given by,

$$\upsilon_r = \frac{Dfs}{4}\left(1 - \frac{d^2}{D^2}\cos^2\alpha\right). \tag{5d}$$

For stationary defect i.e. outer race defect, the load $P(\phi)$ and angular position (ϕ) remains constant. But for the inner race defect and the rolling element defect, point of excitation as well as load at the point of the excitation changes with the time. Load is evenly distributed and can be expanded in the Fourier series as,

$$P(\phi) = p_0 + \sum_r p_r \cos\ r\phi. \tag{6a}$$

where,

$\phi = ft$; and f is the frequency depends upon defect location. The p_0 & p_r are the Fourier coefficients and as explained in the reference [8], they can be written as;

$$P_0 = \frac{1}{T}\int_{-T/2}^{T/2} P(\phi)dt$$

&

$$P_r = \frac{2}{T}\int_{-T/2}^{T/2} P(\phi)\cos\ r\phi dt \tag{6b}$$

Now from equation (2), for non zero value of $P(\phi)$, $[(1-\cos\ \phi)/2\varepsilon] < 1$. Hence, equation (2) can be expanded in binomial series as,

$$P(\phi) = P_{\max}[B_0 + B_1\cos\ \phi + B_2\cos\ 2\phi + B_3\cos\ 3\phi]. \tag{6c}$$

So from equation (6b),

$$P_0 = \frac{P_{\max}}{\pi}[B_0\phi_1 + B_1\cos\ \phi_1 + B_2\cos\ 2\phi_1 + B_3\cos\ 3\phi_1].$$

&

$$P_r = \frac{P_{\max}}{\pi}[\frac{2B_0}{r}\sin\ r\phi_1 + B_1\left\{\frac{\sin(r+1)\phi_1}{(r+1)} + \frac{\sin(r-1)\phi_1}{(r-1)}\right\} + B_2\left\{\frac{\sin(r+2)\phi_1}{(r+2)} + \frac{\sin(r-2)\phi_1}{(r-2)}\right\} + B_3\left\{\frac{\sin(r+3)\phi_1}{(r+3)} + \frac{\sin(r-3)\phi_1}{(r-3)}\right\}]$$

. (6d)

Where,

$$B_0 = 1 - \frac{n}{2\varepsilon} + \frac{n(n-1)}{8\varepsilon^2}\times\frac{3}{2} - \frac{n(n-1)(n-2)}{48\varepsilon^3}\times\frac{5}{2}$$

$$B_2 = \frac{n(n-1)}{8\varepsilon^2}\times\frac{1}{2} - \frac{n(n-1)(n-2)}{48\varepsilon^3}\times\frac{3}{2}$$

$$B_1 = \frac{n}{2\varepsilon} - \frac{n(n-1)}{8\varepsilon^2}\times 2 + \frac{n(n-1)(n-2)}{48\varepsilon^3}\times\frac{15}{4}$$

$$B_3 = \frac{n(n-1)(n-2)}{48\varepsilon^3}\times\frac{1}{4}$$

VI. Calculation of the Forces of Excitation

During the experimentation the transducer will be probably placed on the housing and senses the vibrations of the outer ring only. Hence the solution has been obtained for amplitudes of vibration of mass m_2 for the defect on the different bearing elements.

A. A Defect on the Outer Ring

Consider the single defect on the outer ring of the bearing at angular position of ψ with respect to the transducer. The

interaction of this defect with rolling element causes the force $Q_2(t)$ to be excited. Hence $Q_1(t)$ is assumed to be zero. So from the equation (5a),

$$Q_2(t) = q(t)P(\psi)\cos\psi. \quad (7a)$$

The generated pulse $q(t)$ has periodicity of f_o & can be obtained from equation (5b). The load at angle ψ i.e. $P(\psi)$ can be obtained from equation (2). Hence the excitation force $Q_2(t)$ *i.e* $Q_2(f_o)$ is calculated by putting above values in equation (7a).

B. A Defect on the Inner Ring

The interaction of the single defect on inner ring with rolling element cause excitation of force $Q_1(t)$ & force $Q_2(t)$ can be assumed zero. Under this condition the pulses are generated at inner race defect frequency f_i & defect itself moves at the shaft frequency f_s .The excitation force can be expressed as from equation (5a) as,

$$Q_1(t) = q(t)P(f_s t)\cos f_s t. \quad (8a)$$

The generated pulse $q(t)$ has periodicity of f_i & can be obtained from equation (5b).

The load P having periodicity of f_s & can be obtained from equation (6a) as,

$$P(f_s t) = p_o + \sum_r p_r \cos r f_s t. \quad (8b)$$

The Fourier constants p_0 & p_r are obtained as explained in the equation (6d). Where $\phi_1 = f_s \times T/2$.

Hence the excitation force $Q_1(t)$ is calculated by putting above values in equation (8a).

The excitation force vector for an inner race defect is sum of harmonic components having the same frequency as that of $Q_1(t)$.

C. A Defect on the Ball

The defect on rolling element strikes both inner & outer race. Rolling element revolves about its own axis at frequency f_b and rotates at cage speed of f_c . $Q_1(t)$ & Q_2(t) are excited due to interaction of defect with inner race and outer race respectively. Defect strikes to inner race with frequency f_b and given by equation (5a) as,

$$Q_1(t) = q(f_b t)P(f_c t)\cos f_c t. \quad (9)$$

The expression for the pulse $q(f_b t)$ having periodicity f_b can be obtained from equation (5b) and Fourier constants are obtained from equation (5c).

The load P, having periodicity of f_c & can be obtained from equation (6a).

The Fourier constants p_0 & p_r are obtained as explained in the equation (6d). Where $\phi_1 = f_c \times T/2$.

The defect on rolling element strikes outer race after time pulse π / f_b from the excitation after $Q_1(t)$. But this time period will not have significant effect on P & position $f_c t$ of rolling element. Hence $Q_2(t)$ is given by;

$$Q_2(t) = q(f_b t + \pi)P(f_c t)\cos f_c t. \quad (10)$$

Hence the excitation forces are calculated by putting above values in equation (9) & (10). The pulse generated by interaction of defect with inner race and outer race are assumed to be have same amplitude and nature.

After the necessary assumptions and solving the number of equations obtained in section V, the various values are obtained. After feeding these values in to computer program, numerical results for vibratory amplitude of the mass m_2 i.e. housing can be obtained. These values are plotted as amplitude vs frequency.

VII. Analysis and Solution

The expressions were developed in the preceding sections for the amplitude of the impulses produced at the location of the defect in a bearing under radial load. This gives an expression for the amplitude of the demodulated response produced at the transducer by a defect in a bearing under radial load.

Consider a rolling element bearing with a single point defect on its inner ring, outer ring and rolling element. At time t = 0, the defect is in contact with one of the rolling elements and lies at the centre of the load zone on the line of action of the applied radial load. A vibration transducer is fixed on the bearing in the centre of the load zone with its sensitive axis parallel to the applied load. The mechanical system is symmetrical about the line of the applied load.

In order to obtain the numerical results for the amplitudes of acceleration and velocity of the housing, an 6204 deep groove ball bearing with normal clearance has been considered. Dimensions of the 6204 bearing are as follows: 20 mm bore; 47 mm outside diameter; and 33 mm pitch diameter. They have 8 balls each of 7.95 mm diameter. The nominal contact angle is 0(zero) degree. A diametral clearance of 0.05mm has been considered in the present study. The bearing has been assumed to be mounted on a shaft rotating at higher speed of 6000 rpm and operating at a radial load of 25 kg. For the bearing geometry and spindle speed as mentioned above, the important frequency components and characteristics defect frequencies f_s, f_o, f_i, f_c, f_b, & f_{bd} as explained in section IV are 100Hz, 303.64Hz, 496.36Hz 37.955Hz,195.502 and 391.024Hz respectively. The different sections of the extended portion of the shaft shown in Fig. 1 have lengths of 25mm each. The diameters of the corresponding sections are 30, 25, 20 mm. With the help of these dimensions and following the procedure discussed in section III, the elements of the mass, stiffness and damping matrices can be obtained. A computer program has been developed, which generates the mass, stiffness and damping matrices from these elements and also calculates the elements of the excitation force vectors for various types of localized defects following the procedure discussed in sections V and VI. The program then computes the amplitudes of acceleration of the vibrations of the housing for significant frequency components with the help of the matrix inversion method. The results, thus obtained, have

been plotted in Figures.

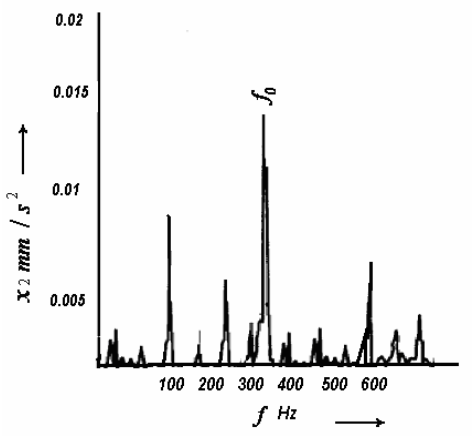

Fig. 7a Amplitude vs frequency for outer ring defect at $\phi = 0$ and defect width 0.5mm

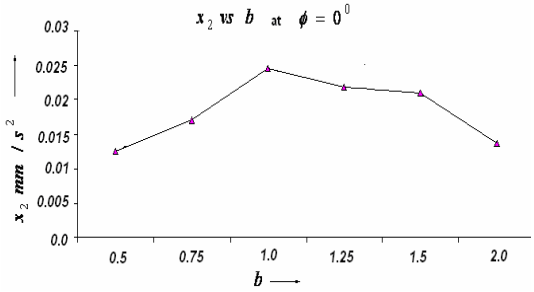

Fig. 7b Amplitude vs defect width for outer ring defect at $\phi = 0$

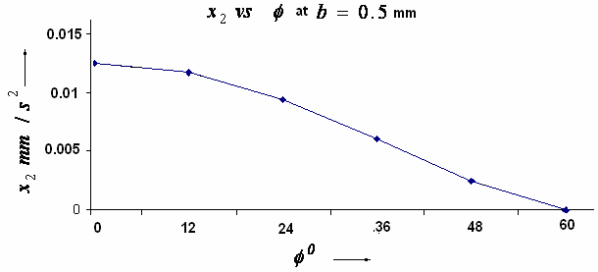

Fig. 7c Amplitude vs defect position for outer ring defect at defect width of 0.5 mm

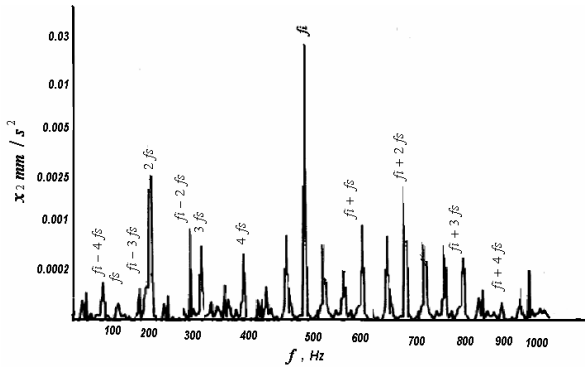

Fig. 8a Amplitude vs frequency for inner ring defect at defect width of 0.5 mm

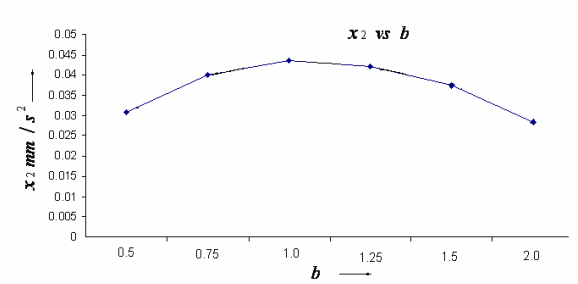

Fig. 8b Amplitude vs defect width for inner ring defect at $\phi = 0$

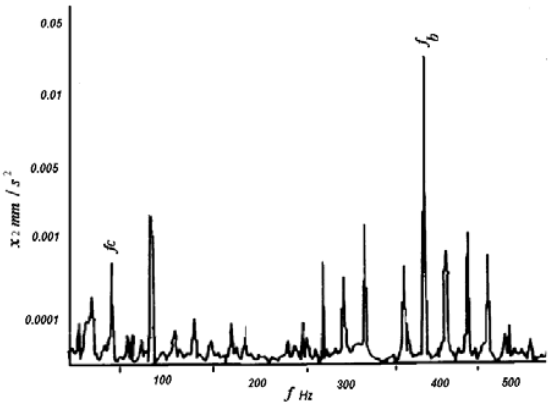

Fig. 9a Amplitude vs frequency for defect on a ball at defect width of 0.5 mm

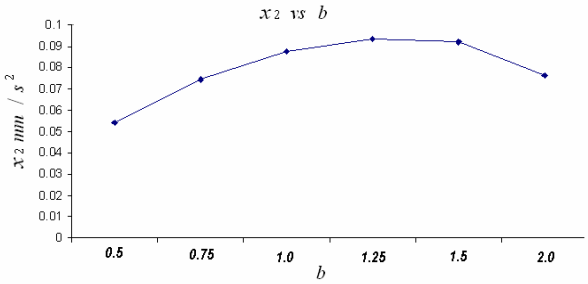

Fig. 9b Amplitude vs defect width for defect on a ball at $\phi = 0$

When the defect is in outer ring, the amplitude vs frequency graph shows the peak at outer ring defect frequency. In Fig. 7a, it is clearly observed that the peak amplitude is observed at outer ring defect frequency and its multiples. The magnitude of the amplitude has a great impact on the position of the defect. As the location of the defect varies with respect to the transducer in the load zone, the peak of amplitude varies and becomes zero outside load zone as shown in Fig. 7c. Whereas Fig. 7b gives variation in the amplitude with the variation in defect size. It is also clear from Fig. 7b that the maximum amplitude is observed when the size of defect is 1mm. Fig. 8a depicts the plot of amplitude vs frequency for the defect on the inner ring. As the inner ring is rotating at the shaft speed, the shaft rotation frequency and its multiples are also observed. In this case the inner race defect frequency amplitude shows the highest in all the peaks. The peak

amplitude varies with the size of inner ring defect as shown in the Fig. 8b. It also depicts maximum value of the peak at defect size of 1 mm as like in Fig. 7b. When the defect is on the ball, it strikes with the outer ring as well as inner ring. The number of balls are moving with the cage speed. The amplitude of the cage frequency and its multiples are as shown in the Fig. 9a. The amplitude of the ball defect frequency is the highest amongst all the peaks. As like outer ring and inner ring defect, the peak amplitude of the ball defect also varies with the defect size as shown in the Fig 9b. The comparison has been made for all above graphs and it is clear that the level of vibrations due to defect in rolling element are much higher than due to defects in outer ring and inner ring. The values of the amplitudes predicted above are theoretical and there may be slightly variation with exact values. Whereas the efforts carried out in the above work can be used to study the approximate amplitude levels of the vibrations at various defect frequencies at comparatively higher speed.

VIII. Conclusion

The characteristic defect frequencies at higher speed are obtained and the corresponding peak amplitudes are noted for deep groove ball bearing. The effort has been carried out in preparing the physical model of the system. The peak amplitudes for the various defect frequencies are observed for the various parameters such as defect size and the position of the defect especially in case of outer ring defect. In case of outer ring defect and inner ring defect, the maximum value of peak is for the same defect size where as rolling element defect gives maximum value of the peak at higher defect size. Also the maximum peak amplitude is observed in case of rolling element defect frequency than other defect frequencies. The magnitude of the amplitude has a great impact on the variation of the load. Further study emphasis on the increase in the amplitude levels of the defect frequency with increase in the load at test bearing. Above predicted absolute values may used to compare with the values obtained from the set-up of the rotor bearing system.

References

[1] P. D. Mcfadden And J. D. Smith, "Model For The Vibration Produced By ASingle Point Defect In A Rolling Element Bearing", Journal of Sound And Vibration (1984) 96(L), 69-82.
[2] M F White, ""Rolling Element Bearing Vibration Transfer Characteristics:Effect of Stiffness," ASME J. Appl. Mech., 46, pp. 677–684, 1979.
[3] D. Smith ,"Vibration monitoring of bearings at low speeds, Tribology Int.June 1982,p-139
[4] Igarashi and H. Hamada Bulletin of the Japan Society of Mechanical Engineers 25, 994-1001 (Studies on the vibration and sound of defective rolling bearings ,first report vibration of ball bearings with one defect)1982.
[5] Wardle, F. P., , "Vibration Forces Produced by Waviness of the Rolling Surfaces of Thrust Loaded Ball Bearings Part 1: Theory, Procd.. of the Inst of Mechanical Engg,202, 1988,No.C5,pp305–312.
[6] G.S. Yadava, K.M. Ramakrishna,N. Tandon, "A comparison of some condition monitoring techniques for the detection of defect in induction motor ball bearings", Mechanical Systems and Signal Processing 21 (2007) 244–256.
[7] P.N. Botsaris, "A Preliminary Estimation of Analysis Methods of Vibration Signals at Fault Diagnosis in Ball Bearings," 4th International conference on NDT, Chania, Crete-Greece, 11-17Oct2007.
[8] Harris, T. A., 1966, Rolling Bearing Analysis, John Wiley, New York.
[9] B C Majumdar, "Introduction to Tribology of the Bearings", Ist Edi, Wheeler & Co .Alahabad,1986.
[10] Eschmann, P., 1985, Ball and Roller Bearings-Theory, Design and Application, John Wiley, NY.